Sixth International Conference on Durability of Concrete Structures **Paper Number ICC02**
18 - 20 July 2018
University of Leeds, Leeds, West Yorkshire, LS2 9JT, United Kingdom

Carbonation in Alternative Cementitious Materials: Implications on Durability and Mechanical Properties

P. Alapati and K. E. Kurtis
School of Civil and Environmental Engineering, Georgia Institute of Technology, Atlanta, Georgia, USA

ABSTRACT

Understanding the rate and implications of carbonation on strength and durability in alternative cementitious materials (ACMs) is critical in designing 'green' concretes for intended service lives. In this paper, three commercially available ACMs, including one calcium aluminate cement (CAC), one calcium sulfoaluminate belite cement (CSA), and one alkali-activated binder using class C fly ash (AA), were evaluated against one portland cement (OPC). Thermogravimetric analysis (TGA) and x-ray diffraction (XRD) techniques were used to understand the effect of carbonation on ACM paste composition. Water sorption tests on both carbonated and uncarbonated cement mortar showed a significant reduction in porosity of this OPC and CAC system with carbonation, whereas no significant change in this CSA and AA system. In addition, the carbonation front in concrete made with these ACMs was measured using phenolphthalein and rainbow indicators at regular intervals of exposure to 7% CO_2, and these results are compared to companion concretes made with this OPC. The rate of carbonation in this CAC, CSA and AA system were significantly higher than that of OPC. The carbonation in the systems made with the ACMs in this study results not only in a decrease in pH, which may lead to depassivation on embedded metal reinforcement but is also found to cause decomposition of main strength giving hydration products. Further research is required to understand the effects of carbonation on steel passivation and chloride threshold levels in the ACM systems.

Keywords: Calcium aluminate cement; Calcium sulfoaluminate cement; Calcium sulfoaluminate belite cement; Alkali-activated binder systems.

1.0 INTRODUCTION

The cement industry emits around 900 kg of carbon dioxide (CO_2) for every 1000 kg of cement it produces, making it one of the two largest producers of industrial CO_2 (Mahasenan *et al.*, 2002). Recent initiatives promoting the sustainability of concrete industry provided momentum for the evaluation of new binding materials that can completely replace the traditional Portland cement. Many alternative cementitious materials (ACM) are known to be sustainable because of lower CO_2 emissions during production and due to their superior properties. For example, manufacturing CSA and CAC cement result in around 30% and 15% reduction in CO_2 emissions (Burris *et al.*, 2015). ACMs also have been used in applications where their unique properties such as high early strength development, high later age strengths, low shrinkage, superior durability are of value. Calcium aluminates, calcium sulfoaluminates, alkali-activated alumino-silicates have shown feasibility for partial or full replacement of portland cement in lab scale studies, but the understanding of long-term performance and durability is limited. Carbonation resistance is a vital durability parameter as it is often associated with corrosion of steel reinforcement embedded in concrete and shrinkage. Many of these ACMs have different cement chemistry which leads to different hydration products, and in turn, can affect the carbonation mechanisms.

The main phases present in a typical portland cement are C_3S, C_2S, C_3A, C_4AF, and $C\overline{S}H_{0.5}$. The dissolution and reaction of these phases with water, not only form the main hydration products (CSH, ettringite, monosulfate, calcium hydroxide), but also some minor constituents of Na_2O and K_2O in the pore solution. The CSH phase is the main strength giving component, whereas the calcium hydroxide (portlandite) along with these oxides of sodium and potassium are mainly responsible for the alkalinity of portland cement systems. Concrete alkalinity helps to maintain the steel reinforcement in passive state limiting corrosion rate. Carbonation, which occurs when CO_2 in the presence of moisture reacts with the calcium-bearing phases in concrete to form calcium carbonate ($CaCO_3$), causes a reduction in the pH of the pore solution and sometimes dissociation of the strength-giving hydration products. $CaCO_3$ formed from the carbonation of portlandite usually precipitates in the concrete pores. Typical reaction mechanism of carbonation in traditional OPC system is shown in Equation 1 (i, ii). Carbonation reduces pH of the concrete in the carbonated zone, due to the reduction in the soluble portlandite phase and formation of insoluble $CaCO_3$, as well as potentially acidic H_2CO_3 (Huet *et al.*, 2011).

$$CH + CO_2 \rightarrow CaCO_3 + H \quad (1\text{-i})$$
$$CO_2 + 2H \rightarrow H_2CO_3 \quad (1\text{-ii})$$
(1)

1.1 Calcium Sulfo-Aluminate Cement (CSA)

The main phases present in a typical CSA cement are $C\overline{S}$ (anhydrite) and $C_4A_3\overline{S}$ (Ye'elimite) (Geng *et al.*, 2014). The possible hydration reactions/products occurring depends on the amount of anhydrite and the presence of portlandite in the cement. If there is sufficient anhydrite present in the cement, reactions (i) and (ii) in Equation 2 occur, forming ettringite as the main hydration product and aluminum hydroxide. Whereas reaction (iii) (Equation 2) will be dominant if there is insufficient anhydrite present in the cement leading to the formation of monosulfate instead of ettringite (Glasser & Zhang, 2001; Winnefeld & Barlag, 2010). With CSA cements also containing C_2S phase, a fourth reaction (iv) in Equation 2 is also possible if there is excess calcium hydroxide present along with excess amounts of anhydrite, forming expansive ettringite (Zhou *et al.*, 2006).

$$C_4A_3\overline{S} + 2C\overline{S} + 38H \rightarrow Ettringite + 4AH_3 \quad (2\text{-i})$$
$$3CA + 3C\overline{S} + 38H \rightarrow Ettringite + 4AH_3 \quad (2\text{-ii})$$
$$3C_4A_3\overline{S} + 18H \rightarrow monosulfate + 2AH_3 \quad (2\text{-iii})$$
$$C_4A_3\overline{S} + 8C\overline{S} + 6CH + 90H \rightarrow 3\,Ettringite \quad (2\text{-iv})$$
(2)

CSH and ettringite are the main hydration products in CSA cement. With no or low C_3S phase being present in the CSA cement and as all the CSH is formed from the C_2S reaction, the amount of portlandite formed is low compared to traditional portland cement systems. Also, the portlandite can be consumed back in the reaction forming just the ettringite. Since the amount of portlandite present in the CSA system is significantly lower than the traditional portland systems, the carbonation mechanisms in CSA systems can be considerably different. The ettringite phase decomposes significantly due to carbonation in CSA systems (Equation 3) causing a reduction in the strength of the matrix. With ettringite being one of the main hydration products and strength giving components (rather than CSH), the long-term stability and the added rapid rate of carbonation is a concern for many researchers (Grounds *et al.*, 1988; Nishikawa *et al.*, 1992). However, an accelerated carbonation study performed in the laboratory (at 20% CO_2 and 70% RH) showed no significant difference in the carbonation depths between CSA and portland cement concrete mixtures (Geng *et al.*, 2014; Zhang *et al.*, 1996).

$$Ettringite + CO_2 \rightarrow 3CaCO_3 + 3C\overline{S} + AH_3 + 29H$$
(3)

1.2 Calcium Aluminate Cement (CAC)

CA, C_3A, C_4AF, and C_2S are the main phases (sometimes the only phases) present in calcium aluminate cement (CAC). The nature of hydration products formed on reaction with water greatly depends on the temperature of hydration. At lower temperatures CAH_{10} forms [reaction (i) in Equation 4], with C_2AH_6 and C_3AH_6 [reaction (ii) and (iii) in Equation 4] being the dominant hydration product at intermediate and higher hydration temperatures respectively, with C_3AH_6 being the most stable product. Over time, the unstable lower dense CAH_{10} and C_2AH_8 convert to highly dense C_3AH_6, leading to higher porosity and a significant reduction in strength (Chotard *et al.*, 2003; Cong and Kirkpatrick, 1993; Scrivener *et al.*, 1999).

$$6CA + 60H \rightarrow CAH_{10} \quad (4\text{-i})$$
$$6CA + 60H \rightarrow 3C_2AH_8 + 3AH_3 + 27H \quad (4\text{-ii})$$
$$6CA + 60H \rightarrow 2C_3AH_6 + 4AH_3 + 36H \quad (4\text{-iii})$$
(4)

Like CSA cement, no C_3S phase is present in the CAC, and if C_2S is present, all the CSH is formed from its reaction, resulting in low amounts of portlandite in the hydrated matrix; thus lower pH in the system and different carbonation mechanisms compared to the traditional portland cement. The possible mechanisms of carbonation in CAC is given in reaction (i) and (ii) of Equation 5. The occurrence of either of the reaction greatly depends on the ease of water evaporation or diffusion to other sources (Goñi *et al.*, 2002). Thermodynamically, reaction (i) (Equation 5) is favored, as the higher liberation of water from reaction (ii) (Equation 5) can inhibit the carbonation reaction. The dissolution of CAH_{10} phase buffers the pore solution, and with carbonation of this phase, it can result in significant reduction in the pH of the system (Fernández-Carrasco *et al.*, 2012; Goñi *et al.*, 2002).

$$CO_2 + CAH_{10} \rightarrow CaCO_3 + 2AH_3 + 7H \quad (5\text{-i})$$
$$CO_2 + 4CAH_{10} \rightarrow C_4AcH_{11} + 6AH_3 + 25H \quad (5\text{-ii})$$
(5)

1.3 Alkali-Activated Cement (AA)

The type of hydration products formed in the AA systems greatly depends on the type of precursor material and the ratio of SiO_2/Na_2O in activator solution. In a calcium-rich precursor such as blast furnace slag and class C fly ash, the main hydration products include (C-A-S-H) type gel, (N-A-S-H) type gel, and (C-S-H) gel; and some minor phases such as Ettringite, Afm type phases and Stratlingite (Ben Haha *et al.*, 2011; Myers *et al.*, 2013; Wang *et al.*, 1995). The carbonation mechanisms also greatly depend on the type of precursor and composition of activator solution. In general, carbonation in AA systems involve decomposition of C-S-H phase to $CaCO_3$ and calcium silicate, and carbonation of NaOH and Na-silicates to sodium carbonate, sodium bicarbonate and their hydrates (Bakharev *et al.*, 2001; Bernal *et al.*, 2012, 2013; Pouhet and Cyr, 2016; Ul Haq *et al.*, 2014).

1.4 Research significance

Understanding the long-term durability performance such as carbonation resistance of the ACM systems is essential in designing 'green' alternatives to traditional Portland cements for intended service lives. Even though prior research exists in understanding the carbonation mechanisms/ reactions of the ACMs, further research is required to better understand its effects on microstructure, porosity and pH of these systems. This paper verifies and provides new insights into the carbonation mechanisms in commercially available CSA, CAC and AA cements and evaluates the implications of carbonation on phase composition, porosity and pH in these systems against one traditional OPC system.

2.0 MATERIALS AND METHODS

Three commercially available ACMs including one calcium aluminate cement (CAC); one calcium sulfoaluminate belite cement (CSA); and one alkali-activated binder system (AA) consisting of class C fly ash and a proprietary two-part activator solution, were evaluated against one ASTM C150 Type I/II portland cement (OPC). Oxide composition and specific gravity of all the binders are shown in Table 1. A 99% pure grade anhydrous citric acid was used to retard the setting time in CSA cement (Burris and Kurtis, 2018). A polycarboxylate-based high range water reducer (HRWR1) by GCP (trade name ADVA 195) was used to achieve desirable slumps in OPC and CSA concrete mixtures. Whereas, a proprietary plasticizer (HRWR2), which also acts as set retarder was used in CAC concrete mixture. A standard ASTM 20-30 test sand from Humboldt Mfg. Co. conforming to ASTM C778 specification was used in making all mortar mixtures. Crushed granitic gneiss coarse aggregates from Vulcan Materials Company (Lithia Springs, Georgia) conforming to ASTM C33 #67 gradation, and river sand from the Lambert Sand and Gravel Plant (Shorter, Alabama) with gradation conforming to ASTM C33 specification were used in making all concrete mixtures.

Cement paste, mortar, and concrete samples were used to test for microstructure, water sorption, and carbonation front respectively. The cement paste mixtures (shown in Table 2) were mixed in a high shear mixer according to ASTM C1738-14 at w/c of 0.45 (0.25 for AA). The set modifier/ activator dosages were chosen so that the corresponding concrete mixes had a workable window of at least 60 min. All the mortar mixes (Table 3) were mixed in Hobart mixer at w/b of 0.45 (AA1 at 0.25 w/b), and sand/binder of 2.75. The sand content was adjusted to account for the differences in the specific gravity of all the ACMs compared to OPC, to have the same volume of binder in all the mortar mixes. The water dosage was also adjusted to account for the sand absorption. The concrete mixes were machine mixed according to ASTM C192-14 at w/b of 0.4 (AA1 at 0.2055 w/b as per manufacturer recommendations). The detailed concrete mixture proportions are shown in Table 4. The admixture/ activator dosages were chosen so that the concrete had a slump of at least 3 inches after 60 minutes of addition of water.

Table 1. Oxide composition and specific gravity of ACMs compared to OPC

Oxide	OPC	CAC	CSA	AA
SiO_2	17.4	5.5	9.9	35.6
Al_2O_3	4.9	45.2	19.8	18.8
Fe_2O_3	4.7	6.9	2.2	6.2
CaO	65.2	37.7	45.8	24.5
MgO	1.4	0.2	1.6	5.7
P_2O_5	0.1	0.1	0.2	0.9
SO_3	2.5	0.1	17.7	2.3
K_2O	0.5	0.3	0.4	0.5
Na_2O	0.5	0.0	0.3	1.8
TiO_2	0.4	2.1	0.7	1.5
Mn_2O_3	0.1	0.0	0.1	0.0
SrO	0.2	0.0	0.1	0.4
ZnO	0.0	0.0	0.1	0.0
Cr_2O_3	0.1	0.1	0.1	0.0
CO_2	0.57	0.24	0.50	0.08
LOI*	2.12	1.86	1.22	1.81
Specific gravity	3.05	2.97	2.81	2.58

*includes CO_2

Table 2. Cement paste mixture proportions

Cement	w/b	Set modifier/ activators (by weight of cement)
OPC	0.45	–
CAC	0.45	–
CSA	0.45	citric acid - 2%
AA	0.25	activator 1 - 2.47%, activator 2 - 2.21%

2.1 Microstructure Analysis

Microstructure analysis was carried out on powdered cement paste samples, both carbonated and uncarbonated. Cement paste cubes of dimension 12.7 mm were prepared according to mixture proportions shown in Table 2, and cured for 28 days at 23 ºC and 100% RH. After curing, some of the samples were exposed to 7% CO_2 at 55% Rh and 30 ºC for 56 days (carbonated), and the other samples were stored in airtight container for the same period (uncarbonated).

Table 3. Cement mortar mixture proportions

Cement	w/b	Admixtures/ activators (by weight of cement)	Cement (g)	Water (g)	Sand (g)
OPC	0.45	–	100	45	275
CAC	0.45	–	100	45	273
CSA	0.45	citric acid - 2%	100	45	268
AA	0.25	activator 1 - 2.47%, activator 2 - 2.21%	100	25	259

Table 4. Concrete mixture proportions

Cement	w/b	Admixtures/ activators (by weight of cement)	Cement (kg/m^3)	Water (kg/m^3)	Sand (kg/m^3)	#67 aggregate (kg/m^3)
OPC	0.40	HRWR1 - 3.5 ml/kg	454	189	703	1056
CAC	0.40	HRWR1 - 1.6 ml/kg	454	189	693	1056
CSA	0.40	citric acid - 2%, HRWR2 - 3.0 ml/kg	454	189	656	1056
AA	0.205	activator 1 - 2.47%, activator 2 - 2.21%	488	109	811	1056

Prior to testing microstructure, the paste samples, both carbonated and uncarbonated, were ground and sieved to a particle size less than 300 microns, and the free water was removed using solvent exchange procedure (Zhang and Scherer, 2011). 5 g of powdered sample was mixed in 50 ml of isopropyl alcohol, and the suspension rests for 15 min. Then, the suspension is filtered using Büchner funnel and a vacuum pump for 5 min, and later, it is washed with 10 ml of diethylene ether for 1 min, during which the vacuum pump is turned off. The resulting suspension is again filtered under vacuum for five more minutes, or until the suspension is dry, whichever is longer. The dried sample is sealed in a small sealed plastic bag and stored in airtight container.

Thermogravimetric Analysis (TGA)

A Hitachi simultaneous thermogravimetric analyzer STA7300 was used to carry out the thermogravimetric measurements. Approximately, 20 mg of sample with the particle size less than 74 microns, is taken in an open 70 μl platinum crucible and dried in TG at 25 ºC under a constant stream of Nitrogen (N_2) gas for 15 min, or until the constant mass, whichever is longer. Later the temperature is increased to 40 ºC and held constant for 5 min. Then, the sample was heated from 40 to 1000 ºC, at a rate of 10 ºC/min, and the data is recorded at a rate of 120 data points per minute. During measurement, N_2 was used as a protective gas with a flow rate of 100 Cc/min.

X-ray Diffraction (XRD)

A PANalytical Empyrean diffractometer with Bragg–Brentano HD X-ray mirror and goniometer radius of 240 mm was used for data collection. The sample was incident with CuKα X-rays generated using Empyrean Cu LFF HR X-ray tube at 45 KV and 40 mA operating conditions. Soller slits of 0.04 rad and the fixed Mask, anti-scatter, and divergence slits of 4 mm, 1 º, and ¼ º were used in the incident beam path. In the diffracted beam path, a fixed anti-scatter slit of 7.5 mm and soller slits of 0.04 rad were used. A PIXcel3D-Medipix3 1x1 area detector with an active length of 3.347 º was used for data acquisition. Data was collected over an angular range of 5 º to 70 º with a step size and counting time of 0.013 º and 16.32 s respectively, resulting in a total measurement time of less than 7 min.

The powdered samples with particle dimension less than 149 microns were backloaded into the sample holder with an opening diameter of 17 mm. Phase identification was carried out using PANalytical X' Pert High Score plus v4.5 using PDF-4+ 2017 material identification database by International Center for Diffraction Data.

2.2 Water Sorption

The initial and secondary water sorptivity rate was determined on cement mortar discs, averaged from two test specimens. The cylinders were cast according to mix proportions given in Table 3 and cured at 23 ºC and 100% RH for 28 days. Then they are cut into discs of 76 mm in diameter and thickness of 38 mm using a wet tile saw. Later, the mortar discs were further cured for an additional 28 days at 55% RH, and epoxy coated on all sides except one end of the flat surface. After the epoxy coat dried, the uncoated side of the sample was exposed to water with 1 to 2 mm of the sample immersed. The uptake of water is measured by weighing the specimens at intervals of 30 min, 60 min, every hour until 6 hours to determine initial sorption rate; and once a day up to 7 days to determine secondary sorption rate. The sorption rate ($mm/s^{0.5}$) is measured using the slope of the line that is the best fit to water absorption plotted against the square root of time ($s^{0.5}$).

After measuring the sorptivity rates on uncarbonated samples, they were vacuum dried for 4 hours and stored at 55% RH and 23 ºC for additional 28 days. Then the mortar discs are carbonated by exposing them to 7% CO_2 at 55% RH and 30 ºC for 56 days, and the sorptivity measurements were carried out

once again to determine the initial and secondary sorption rates in the carbonated samples.

2.3 Carbonation Front and pH Profile Measurement

Concrete cylinders of 152 mm diameter and 305 mm height were cast according to mixture proportions shown in Table 4 and cured for 28 days at 23 ºC and 100% RH. Then they were cut into two pieces using a wet tile saw, resulting in cylinders with dimensions 152 mm diameter and 150 mm height. The samples were further cured for an additional 28 days at 23 ºC and 55% RH.

After the curing regime, the concrete samples were exposed to 7% CO_2 at 30 ºC and 55% RH for 0, 3, 7, 14, 21, 28, 42, 56, and 84 days. At the end of the exposure, the samples were split into two halves along the major axis and sprayed with 1% phenolphthalein indicator on the split surface of one half, and with a commercially available 'rainbow indicator' (sourced from Germann Instruments) on the other half. Carbonation front was determined by averaging the carbonation depths measured based on the color change with the phenolphthalein and rainbow indicator, with five measurements taken on each side of the curved surface. Also, based on the color profile achieved with the rainbow indicator, the pH levels were estimated in both carbonated and uncarbonated regions.

3.0 RESULTS AND DISCUSSIONS

3.1 Effect of Carbonation on Paste Composition

The thermogravimetric analysis results of all the cement paste mixtures, both carbonated and uncarbonated are shown in Fig. 1 (a to d); and the XRD peaks of OPC, CAC, CSA, and AA are shown in Fig. 2 to Fig. 5 respectively. In OPC mixture, with carbonation, there is a reduction in the DTG peaks of portlandite, ettringite, and monosulfate phases, suggesting carbonation of not only the portlandite phase but also ettringite and monosulfate phases. However, even after exposure to 7% CO_2, there is still a significant amount of portlandite present, which can maintain the pH in the system. The XRD plot of carbonated cement paste shows $CaCO_3$ with two polymorphs, calcite, and vaterite. Vaterite is usually formed with the carbonation of CSH phase. It is metastable at room temperature and can readily recrystallize to calcite polymorph when exposed to water.

Unlike OPC, this CAC mixture has no portlandite present in the system, and the carbonation results in the significant decomposition of CAH_{10} phase to $CaCO_3$ (Aragonite and Vaterite) and AH_3 (Gibbsite), suggesting carbonation mechanism similar to reaction (i) in Equation 5. Since CAH_{10} is one of the main strength giving hydration product which also buffers the pore solution, decomposition of CAH_{10} phases due to carbonation in this CAC system can result in significant reduction of both the mechanical properties of the matrix and the pH of the pore solution. No change is observed in the amount of

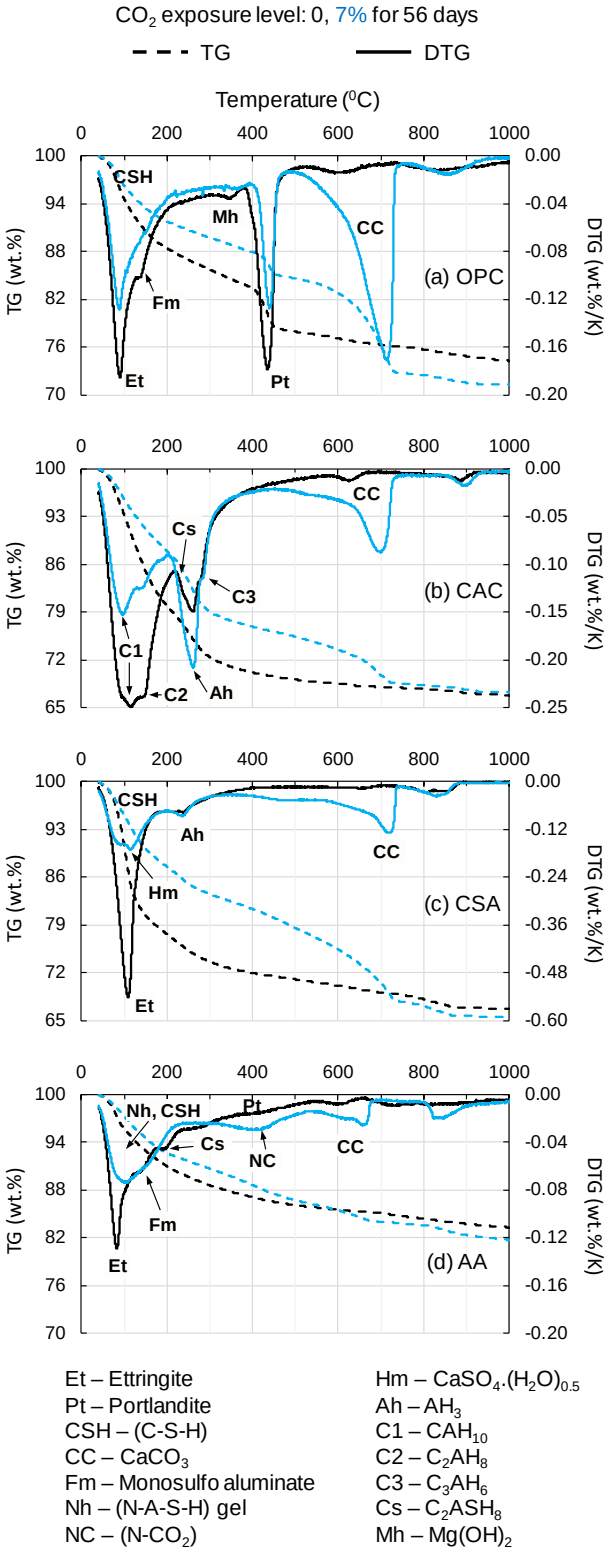

Fig. 1. TG and DTG curves of cement pastes made with (a) OPC, (b) CAC, (c) CSA, and (d) AA; exposed to 0% and 7% CO_2

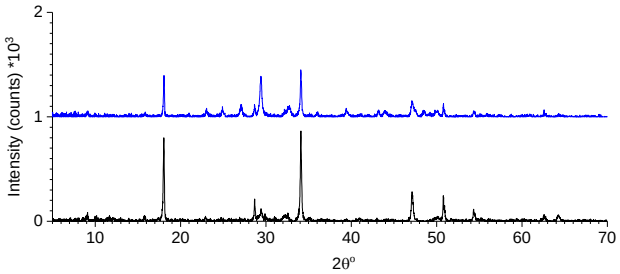

Fig. 2. XRD of cement paste made with OPC, exposed to 0% and 7% CO_2

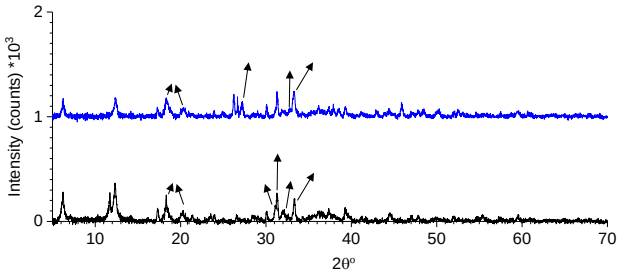

Fig. 3. XRD of cement paste made with CAC, exposed to 0% and 7% CO_2

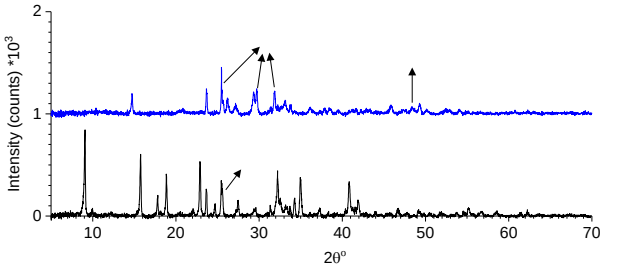

Fig. 4. XRD of cement paste made with CSA, exposed to 0% and 7% CO_2

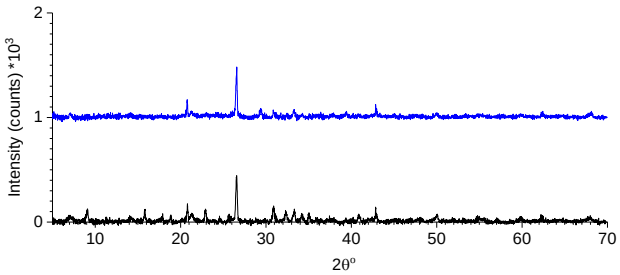

Fig. 5. XRD of cement paste made with AA, exposed to 0% and 7% CO_2

C_3AH_6 phase present in the matrix with carbonation, suggesting that carbonation of the C_3AH_6 phase is less favorable compared to the CAH_{10} phase.

In the CSA matrix, with carbonation, both the DTG and XRD peaks of ettringite disappeared, and the peaks of gibbsite, anhydrite, and hemihydrate increased. This suggests complete decomposition of ettringite according to reaction (i) in Equation 3. Since ettringite is the dominant strength giving phase, the carbonation in this CSA systems can result in significant reduction in mechanical properties in addition to the pH of pore solution.

With carbonation in AA mixture, like the CSA matrix, the ettringite peaks completely disappeared, and a significant reduction in the stratlingite phase can also be observed. However, unlike the CSA matrix, ettringite is not the dominant strength giving phase in AA matrix. (Na–A–S–H) and (C–S–H) are dominant strength giving phases in this AA system, and no significant reduction is observed in these two phases with carbonation. This suggests the reduction in strength in this AA system might be significantly lower when compared to the other ACMs (CAC and CSA). But, the pore solution pH might drop considerably due to the carbonation of alkalis (NaOH) into alkali carbonates (Na–CO_2) – DTG peak at around 400 ºC.

Figure 6 shows the bound CO_2 levels calculated from the TG data in both carbonated and uncarbonated systems. The amount of CO_2 from the decomposition of carbonated phases in carbonated CSA paste mixture is similar to OPC, whereas it is 50% lower in CAC paste mixture and five folds lower in AA paste mixture. The variation in the bound CO_2 levels with cement type is due to the differences in carbonation nature of their hydration products and may not necessarily relate to the extent of carbonation.

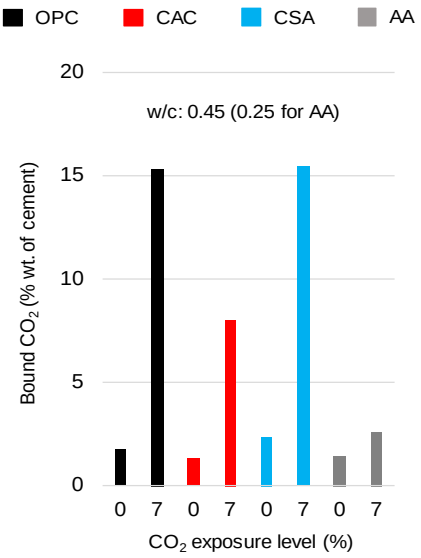

Fig. 6. Bound CO_2 levels in cement paste made with OPC and ACMs, exposed to 0% and 7% CO_2

3.2 Effect of Carbonation on Water Sorption

Figure 7 shows initial and secondary sorption rate of both carbonated and uncarbonated cement mortars made with OPC, CAC, CSA, and AA. Significant reduction in initial sorption rate with carbonation in OPC and CAC mortars suggests precipitation of $CaCO_3$ in the capillary pores. Whereas, increase in secondary sorption rate with carbonation might be due to the significant decomposition of hydration products, thereby increasing gel porosity or porosity in the interfacial transition zone (ITZ). This may be

attributed to the initial dissolution of CH and CAH_{10} phases, followed by carbonation of these phases in pore water and eventually precipitation of the carbonated products (mainly $CaCO_3$), but further study is required to verify this mechanism.

However, with CSA and AA mortars, in contrast to OPC and CAC mortars, a slight increase in initial water sorption and a decrease in secondary sorption with carbonation is observed. This could be due to the filling of carbonated products within the gel or ITZ pores since ettringite and stratlingite are the dominant phases that carbonate in this CSA and AA mortars, and these phases do not readily dissolve in pore water unlike the CH and CAH_{10} phases present in OPC and CAC mixtures respectively.

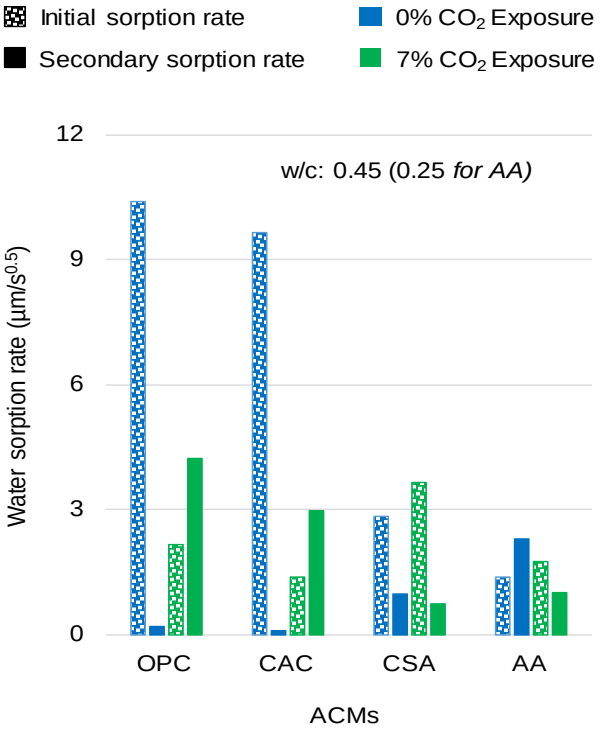

Fig. 7. Initial and secondary sorption rate of cement mortar samples made with OPC and ACMs, exposed to 0% and 7% CO_2

3.3 Carbonation Front and pH Estimates

The mean carbonation front at exposure ages of 0, 3, 7, 14, 21, 28, 42, 56, and 84 days and carbonation rates in mm/yr$^{0.5}$ were measured based on the colour change with the phenolphthalein and rainbow indicator, and are shown in Fig. 8. The pH levels in both carbonated and uncarbonated regions were estimated based on the color change with rainbow indicator and are shown in Table 5. The pH in the uncarbonated region of OPC and AA concrete mixtures was greater than 13, and it is between 9 to 11 in CAC and CSA mixtures – which suggests that even the pre-carbonation environment in CAC and CSA systems may be detrimental to embedded steel passivation. With carbonation, the pH levels dropped to 9-11 in OPC mixture and to less than 9 in CAC, CSA and AA mixtures. Also, the carbonation rate in CAC and CSA mixtures is 3 folds higher than that of OPC mixtures, and the carbonation rate in AA mixture is 50% greater than the CAC and CSA mixtures. OPC mixtures have higher amounts of CH phase in the system, and as observed in the carbonation of paste samples in the previous section, a significant amount of CH phase can still be present even after exposure to higher CO_2 levels, that can buffer the pore solution. So, the carbonation front measured using phenolphthalein and rainbow indicators may not be representative of the actual depth of CO_2 ingress in the system. However, since the passivation of embedded steel reinforcement in concrete systems is dependent on the pH of the system at the interface rather than the CO_2 ingress depth levels, the carbonation rate measured here can provide reasonable estimates of relative performance of these ACM mixtures compared to OPC mixture in resisting depassivation of reinforcement.

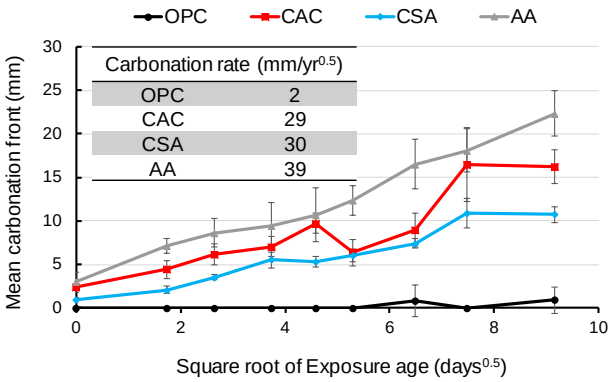

Fig. 8. Mean carbonation front of concrete samples made with OPC and ACMs, exposed to 7% CO_2, at different exposure ages

Table 5. pH levels in both carbonated and uncarbonated regions of concrete samples made with OPC and ACMs, exposed to 7% CO_2 for 84 days

Binder	Carbonated pH	Uncarbonated pH
OPC	9 - 11	> 13
CAC	< 9	9 - 11
CSA	< 9	9 - 11
AA	< 9	> 13

4.0 CONCLUSIONS

The accelerated carbonation tests, along with complementary characterization by TGA and XRD, and water sorptivity measurements performed in this study were intended to understand the carbonation mechanisms and evaluate the performance of commercially available CAC, CSA and AA systems in resisting carbonation compared to OPC systems, and has led to the following conclusions.

- Carbonation in CAC and CSA systems can result in significant decomposition of main hydration products thereby affecting their mechanical properties. Whereas, no significant decomposition of main hydration products is observed in OPC and AA systems.
- Carbonation in OPC and CAC mortar mixtures resulted in significant reduction in capillary porosity, whereas no significant change is observed in CSA and AA mixtures. Further research using other porosity measurement techniques such as mercury intrusion porosimetry is required to validate these results.
- CAC, CSA and AA concrete mixtures carbonated at a much faster rate compared to OPC concrete mixture.
- The pH levels in the carbonated region of ACM concrete dropped below 9 – which may result in significant destabilization of the passive layer in steel reinforcements.

Even though this study allowed to conclude that, unlike the traditional OPC system, carbonation in this CAC, CSA, and AA systems resulted in higher carbonation rates and greater reduction in pH, the authors emphasize the need for further research to better understand the effects of carbonation on steel passivation and chloride threshold levels in the ACM systems.

Acknowledgement

The authors thank Robert Moser (U.S. Army ERDC) for performing the oxide analysis, Molly Canet for her assistance in carrying out some of the experiments, and the other partners involved in this project for their support and discussions: Lisa Burris (Ohio State University), Tyler Ley (Oklahoma State University), Neal Berke (Tourney Consulting Group), and Richard Meininger (USDOT/FHWA). The authors also acknowledge FHWA for funding this research under project number DRFH61-14-H-0000.

References

Bakharev, T., Sanjayan, J. ., & Cheng, Y.-B. (2001). Resistance of alkali-activated slag concrete to carbonation. *Cement and Concrete Research*, *31*(9), 1277–1283. https://doi.org/10.1016/S0008-8846(01)00574-9

Ben Haha, M., Le Saout, G., Winnefeld, F., & Lothenbach, B. (2011). Influence of activator type on hydration kinetics, hydrate assemblage and microstructural development of alkali activated blast-furnace slags. *Cement and Concrete Research*, *41*(3), 301–310. https://doi.org/10.1016/J.CEMCONRES.2010.11.016

Bernal, S. A., Provis, J. L., Brice, D. G., Kilcullen, A., Duxson, P., & Van Deventer, J. S. J. (2012). Accelerated carbonation testing of alkali-activated binders significantly underestimates service life: The role of pore solution chemistry. *Cement and Concrete Research*, *42*(10), 1317–1326. https://doi.org/10.1016/j.cemconres.2012.07.002

Bernal, S. A., Provis, J. L., Walkley, B., Nicolas, R. S., Gehman, J. D., Brice, D. G., … Van Deventer, J. S. J. (2013). Gel nanostructure in alkali-activated binders based on slag and fly ash, and effects of accelerated carbonation. *Cement and Concrete Research*, *53*, 127–144. https://doi.org/10.1613/jair.301

Burris, L. E., & Kurtis, K. E. (2018). Influence of set retarding admixtures on calcium sulfoaluminate cement hydration and property development. *Cement and Concrete Research*, *104*, 105–113. https://doi.org/10.1016/J.CEMCONRES.2017.11.005

Burris, L., Kurtis, K. E., & Morton, T. (2015). *Novel Alternative Cementitious Materials for Development of the Next Generation of Sustainable Transportation Infrastructure*.

Chotard, T. J., Boncoeur-Martel, M. P., Smith, A., Dupuy, J. P., & Gault, C. (2003). Application of X-ray computed tomography to characterise the early hydration of calcium aluminate cement. *Cement and Concrete Composites*, *25*(1), 145–152. https://doi.org/10.1016/S0958-9465(01)00063-4

Cong, X., & Kirkpatrick, R. james. (1993). Hydration of Calcium Aluminate Cements: A solid-state Al NMR study. *Journal of American Ceramic Society*, *76*(2), 409–416. https://doi.org/10.1017/CBO9781107415324.004

Fernández-Carrasco, L., Torréns-Martín, D., & Martínez-Ramírez, S. (2012). Carbonation of ternary building cementing materials. *Cement and Concrete Composites*, *34*(10), 1180–1186. https://doi.org/10.1016/j.cemconcomp.2012.06.016

Geng, H., Duan, P., Chen, W., & Shui, Z. (2014). Carbonation of sulphoaluminate cement with layered double hydroxides. *Journal of Wuhan University of Technology-Mater. Sci. Ed.*, *29*(1), 97–101. https://doi.org/10.1007/s11595-014-0874-y

Glasser, F. P., & Zhang, L. (2001). High-performance cement matrices based on calcium sulfoaluminate-belite compositions. *Cement and Concrete Research*, *31*(12), 1881–1886. https://doi.org/10.1016/S0008-8846(01)00649-4

Goñi, S., Gaztañaga, M. T., & Guerrero, a. (2002). Role of Cement Type on Carbonation Attack. *Journal of Materials Research*, *17*(7), 1834–1842. https://doi.org/10.1557/JMR.2002.0271

Grounds, T., G Midgley, H., & V Novell, D. (1988). Carbonation of ettringite by atmospheric carbon dioxide. *Thermochimica Acta*, *135*, 347–352. https://doi.org/10.1016/0040-6031(88)87407-0

Huet, B., Tasoti, V., & Khalfallah, I. (2011). A review of Portland cement carbonation mechanisms in CO2 rich environment. *Energy Procedia*, *4*, 5275–5282. https://doi.org/10.1016/j.egypro.2011.02.507

Mahasenan, N., Smith, S., & Humphreys, K. (2002). The Cement Industry and Global Climate Change: Current and Potential Future Cement Industry CO2 Emissions. In J. Gale & Y. Kaya (Eds.), *International conference on Greenhouse Gas Control Technologies* (pp. 995–1000). Kyoto, japan: Elsevier Ltd.

Myers, R., Bernal, S., San Nicolas, R., & Provis, J. (2013). Generalized Structural Description of Calcium-Sodium Aluminosilicate Hydrate Gels: The Cross-Linked Substituted Tobermorite Model. *Langmuir : The ACS Journal of Surfaces and Colloids*, *29*.

Nishikawa, T., Suzuki, K., Ito, S., Sato, K., & Takebe, T. (1992). Decomposition of synthesized ettringite by carbonation. *Cement and Concrete Research*, *22*(1), 6–14. https://doi.org/10.1016/0008-8846(92)90130-N

Pouhet, R., & Cyr, M. (2016). Carbonation in the pore solution of metakaolin-based geopolymer. *Cement and Concrete Research*, *88*, 227–235. https://doi.org/10.1016/J.CEMCONRES.2016.05.008

Scrivener, K. L., Cabiron, J.-L., & Letourneux, R. (1999). High-performance concretes from calcium aluminate cements. *Cement and Concrete Research*, *29*(8), 1215–1223. https://doi.org/10.1016/S0008-8846(99)00103-9

Ul Haq, E., Padmanabhan, S. K., & Licciulli, A. (2014). In-situ carbonation of alkali activated fly ash geopolymer. *Construction and Building Materials*, *66*, 781–786. https://doi.org/10.1016/j.conbuildmat.2014.06.012

Wang, S.-D., Pu, X.-C., Scrivener, K. L., & Pratt, P. L. (1995). Alkali-activated slag cement and concrete: a review of properties and problems. *Advances in Cement Research*, *7*(27), 93–102. https://doi.org/10.1680/adcr.1995.7.27.93

Winnefeld, F., & Barlag, S. (2010). Calorimetric and thermogravimetric study on the influence of calcium sulfate on the hydration of ye'elimite. *Journal of Thermal Analysis and Calorimetry*, *101*(3), 949–957. https://doi.org/10.1007/s10973-009-0582-6

Zhang, J., & Scherer, G. W. (2011). Comparison of methods for arresting hydration of cement. *Cement and Concrete Research*, *41*(10), 1024–1036. https://doi.org/10.1016/J.CEMCONRES.2011.06.003

Zhang, L., Wang, Y. M., & Su, M. Z. (1996). Control properties of sulpho- and ferro-aluminate cement with the special admixtures. In *10th I.C.C.C. Proceedings*. Gothenburg, Sweden.

Zhou, Q., Milestone, N. B., & Hayes, M. (2006). An alternative to Portland Cement for waste encapsulation-The calcium sulfoaluminate cement system. *Journal of Hazardous Materials*, *136*(1 SPEC. ISS.), 120–129. https://doi.org/10.1016/j.jhazmat.2005.11.038